Electronic Supporting Information for:

A three-dimensional structure built of paddle-wheel and triazolate-dinuclear metal clusters: synthesis, deformation and reformation of paddle-wheel unit in the single-crystal-to-single-crystal transformation

Feilong Yang, Qingshu Zheng, Zhenxia Chen, Yun Ling,* Xiaofeng Liu, Linhong Weng, Yaming Zhou*

Shanghai Key Laboratory of Molecular Catalysis and Innovative Materials, Department of Chemistry, Fudan University, 220 Handan Road, Shanghai 200433, P. R. China
*Corresponding author: yunling@fudan.edu.cn (Ling, Y.); ymzhou@fudan.edu.cn (Zhou, Y.M.)

1. **Synthesis of H_4BPTC**

H_4BPTC was synthesized according to the route shown in scheme S1.

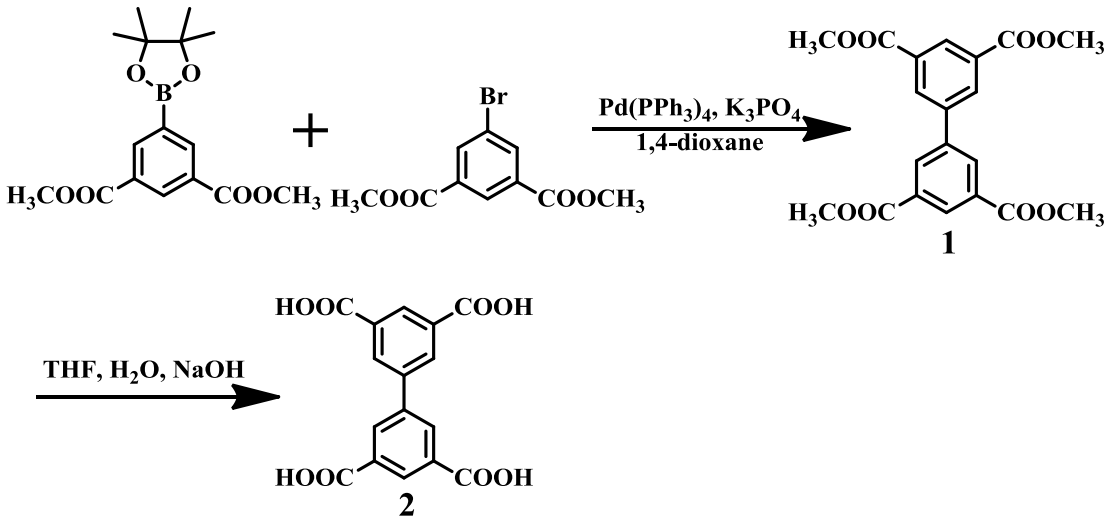

Scheme S1. Synthesis process of the ligand H_4BPTC

The detail procedures are: dimethyl-5-boronic acid pinacol ester-isophtalate[S1] (3.50 g, 11 mmol), dimethyl-5-bromo-isophtalate (3.60g, 13 mmol), $Pd(PPh_3)_4$ (0.69g 0.6 mmol), K_3PO_4 (4.244g, 20mmol) were mixed in a 250 mL flask. The flask was pumped under vacuum for 30 min and 120 mL pure 1,4-dioxane was added. Then the mixture was heated to reflux under nitrogen atmosphere for 24 h. The resulting yellow mixture was filtrated and the filtration was concentrated in vacuum to give crude product, which was then recrystallized in ethyl acetate. Yellow solid products of **1** were collected by filtration (2.95g, 69 %). ^{1}HNMR (400 MHz, $CDCl_3$): 8.73 (s, 2H), 8.52 (s, 4H), 4.00 (s, 12H) ppm.

1 (4 g, 10.4 mmol) was then suspended in a mixture of THF (40 mL) and 10 M NaOH aqueous solution (40 mL). The mixture was stirred at reflux temperature overnight and then THF were removed under the vacuum condition. Dilute HCl was used to adjust the pH to be 3. Solid products was then precipitated and collected by filtration, washed with water, and dried under vacuum condition to give **2** (3.2g, 93 % yield). 1H-NMR (400 MHz, d_6-DMSO): 8.52 (s, 2H), 8.43 (s, 6 H) ppm.

Table S1. Selected bond lengths [Å] and angles [°] for MAC-6, MAC-6' and MAC-6-R

MAC-6			
Zn(1)-N(1)	2.013(3)	Zn(2)-O(4)#4	1.920(3)
Zn(1)-O(1)	2.031(2)	Zn(2)-O(4)#5	1.920(3)
Zn(1)-O(1)#1	2.031(2)	Zn(2)-N(2)	1.975(2)
Zn(1)-O(2)#2	2.070(2)	Zn(2)-N(2)#6	1.975(2)
Zn(1)-O(2)#3	2.070(2)	O(4)-Zn(2)#4	1.920(3)
O(1)-Zn(1)-O(2)#2	157.18(10)	O(4)#4-Zn(2)-O(4)#5	111.0(2)
O(1)#1-Zn(1)-O(2)#2	84.94(12)	O(4)#4-Zn(2)-N(2)	112.46(13)
N(1)-Zn(1)-O(2)#3	100.84(11)	O(4)#5-Zn(2)-N(2)	104.46(11)
O(1)-Zn(1)-O(2)#3	84.94(12)	O(4)#4-Zn(2)-N(2)#6	104.46(11)
O(1)#1-Zn(1)-O(2)#3	157.18(10)	O(4)#5-Zn(2)-N(2)#6	112.46(13)
O(2)#2-Zn(1)-O(2)#3	85.79(17)	N(2)-Zn(2)-N(2)#6	112.25(14)
MAC-6'			
Zn(1)-O(1)	1.934(11)	Zn(3)-O(15)#3	2.018(11)
Zn(1)-N(1)	1.977(14)	Zn(3)-N(3)	2.072(12)
Zn(1)-N(6)	1.977(13)	Zn(3)-O(17)	2.126(11)
Zn(1)-O(5)#1	2.003(12)	Zn(3)-O(4)#1	2.244(10)
Zn(2)-O(13)#2	1.926(11)	Zn(4)-O(11)#4	1.948(11)
Zn(2)-N(7)	1.943(12)	Zn(4)-O(3)#5	1.949(10)
Zn(2)-O(9)	1.972(12)	Zn(4)-O(16)	1.965(13)
Zn(2)-N(2)	2.040(13)	Zn(4)-N(8)	1.977(14)
Zn(3)-O(7)#3	1.975(11)		
O(1)-Zn(1)-N(1)	126.4(5)	O(15)#3-Zn(3)-N(3)	102.4(5)
O(1)-Zn(1)-N(6)	99.3(5)	O(7)#3-Zn(3)-O(17)	91.3(5)
N(1)-Zn(1)-N(6)	109.6(5)	O(15)#3-Zn(3)-O(17)	82.9(5)
O(1)-Zn(1)-O(5)#1	111.1(5)	N(3)-Zn(3)-O(17)	97.5(5)
N(1)-Zn(1)-O(5)#1	107.7(5)	O(7)#3-Zn(3)-O(4)#1	88.4(5)
N(6)-Zn(1)-O(5)#1	99.0(5)	O(15)#3-Zn(3)-O(4)#1	92.9(4)
O(13)#2-Zn(2)-N(7)	122.9(6)	N(3)-Zn(3)-O(4)#1	94.4(4)
O(13)#2-Zn(2)-O(9)	108.8(6)	O(17)-Zn(3)-O(4)#1	168.0(5)
N(7)-Zn(2)-O(9)	110.2(6)	O(11)#4-Zn(4)-O(3)#5	125.6(5)
O(13)#2-Zn(2)-N(2)	98.1(5)	O(11)#4-Zn(4)-O(16)	99.2(5)
N(7)-Zn(2)-N(2)	111.4(6)	O(3)#5-Zn(4)-O(16)	120.6(5)
O(9)-Zn(2)-N(2)	103.3(5)	O(11)#4-Zn(4)-N(8)	105.2(5)
O(7)#3-Zn(3)-O(15)#3	158.0(5)	O(3)#5-Zn(4)-N(8)	102.9(5)
O(7)#3-Zn(3)-N(3)	99.4(5)	O(16)-Zn(4)-N(8)	99.7(6)
MAC-6-R			
Zn(1)-N(1)	2.030(12)	Zn(2)-O(4)#4	1.911(10)
Zn(1)-O(1)	2.033(10)	Zn(2)-N(2)	1.975(9)

Zn(1)-O(2)#2	2.059(10)		
N(1)-Zn(1)-O(1)	100.7(4)	O(1)-Zn(1)-Zn(1)#2	87.7(3)
O(1)-Zn(1)-O(1)#1	96.4(7)	O(4)#4-Zn(2)-O(4)#5	108.3(8)
N(1)-Zn(1)-O(2)#2	101.4(4)	O(4)#4-Zn(2)-N(2)	113.0(5)
O(1)-Zn(1)-O(2)#2	157.3(4)	O(4)#5-Zn(2)-N(2)	105.1(4)
O(1)-Zn(1)-O(2)#3	84.7(5)	N(2)-Zn(2)-N(2)#6	112.5(6)
O(2)#2-Zn(1)-O(2)#3	85.9(6)		

Symmetry codes used for **MAC-6**: #1: x, -y+1, z; #2: -x+1, -y+1, -z+1; #3: -x+1, y, -z+1; #4: -x+1/2, -y+1/2, -z; #5: x-1/2, -y+1/2, z; #6: -x, y, -z.

Symmetry codes used for **MAC-6'**: #1: -x+1, -y+1, -z; #2: x-1, -y+1/2, z-1/2; #3: -x+2, -y+1, -z+1; #4: x, -y+1/2, z+1/2; #5: -x+2, y+1/2, -z+1/2.

Symmetry codes used for **MAC-6-R**: #1: x, -y+1, z; #2: -x+1, -y+1, -z+1; #3: -x+1, y, -z+1; #4: -x+1/2, -y+1/2, -z; #5: x-1/2, -y+1/2, z; #6: -x, y, -z; #7: -x+3/2, -y+1/2, -z+1.

Figure S1. (a) the bptc ligand connects the paddle-wheel and triazolate-dinculear units in *trans*-position in MAC-6 (the structural motif labeled with atomic numbers, symmetry code: A: x, 1-y, z; B: -x, 1-y, -z; C: 1-x, y, 1-z; D: 0.5-x, 0.5-y, -z); (b) the 3D porous structure of MAC-6; (c) the structural motif of closed phase of MAC-6' (symmetry code: A:-1+x, -y, -0.5+z; B: -1+x, y, -1+z; D: x, -y, 0.5+z; E: x, 1-y, 0.5+z; F: 1+x, y, 1+z; G: x, 1-y, -0.5+z; H: x, 1+y, z; I: 1+x, 1-y, 0.5+z); (d) the 3D closed framework of MAC-6'. (cationic guests of $(CH_3)_2NH_2$ and guest molecules are omitted as well as hydrogen atoms are omitted for clarity), (e)-(f) the changes of paddle-wheel units during the phase transformation.

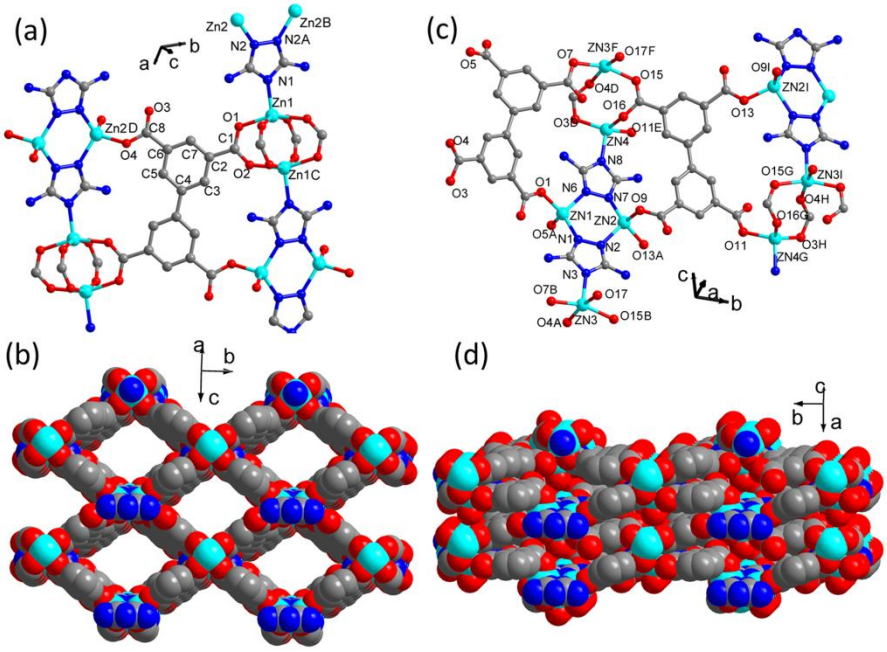

Figure S2. (a) Connolly surface area calculated with probe atomic radii of 1.4 Å; (b) the theoretical accessible surface area calculated with the probe atomic radii of 1.84 Å. (cell parameters: 3×2×3)

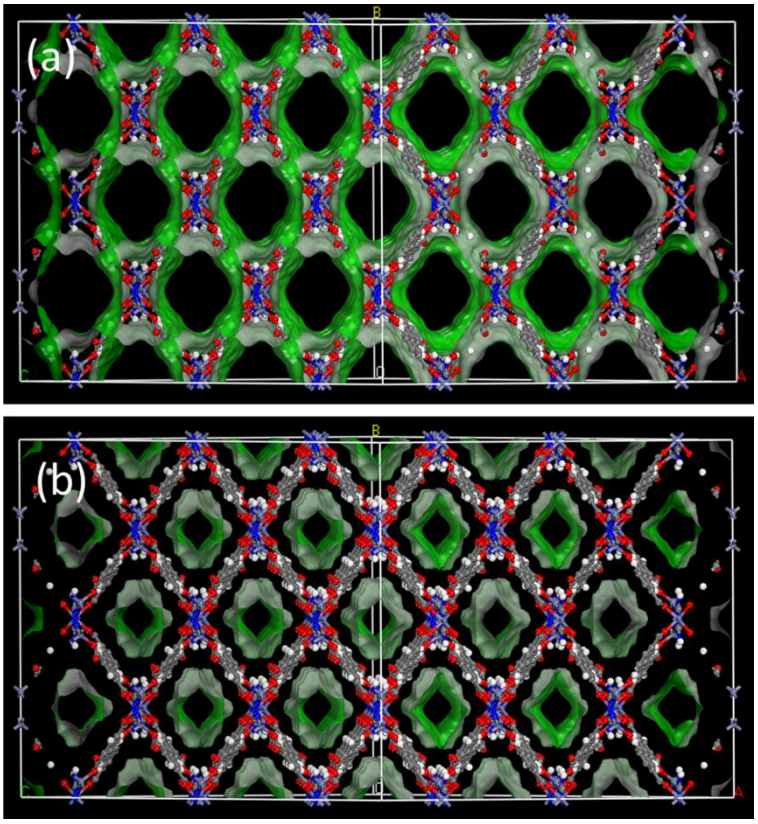

Connolly Surface (Å^2) cell: 3×2×3	Accessible Solvent Surface (Å^2) cell: 3×2×3	Dc (g/cm^3)	Volume (Å^3)
17535.64	10185.28	1.13	3641

$$\text{Theoretical Surface area} = \frac{A.S.S(per\ \ unit\ \ cell)}{D_c \times Volume} \times 10^4 \quad m^2/g$$

MAC-6 is therefore calculated to be 1375 m^2/g

Figure S3. Thermogravimetric analysis (TGA) of MAC-6 (a) and MAC-6' (b) samples. The DSC signal for MAC-6 was also deposited in (a). Because of the phase transformation and the release of parts of guest molecules happens simultaneously from 50 to 120 °C, it is difficult to identify which one contributes the endothermic peak exactly.

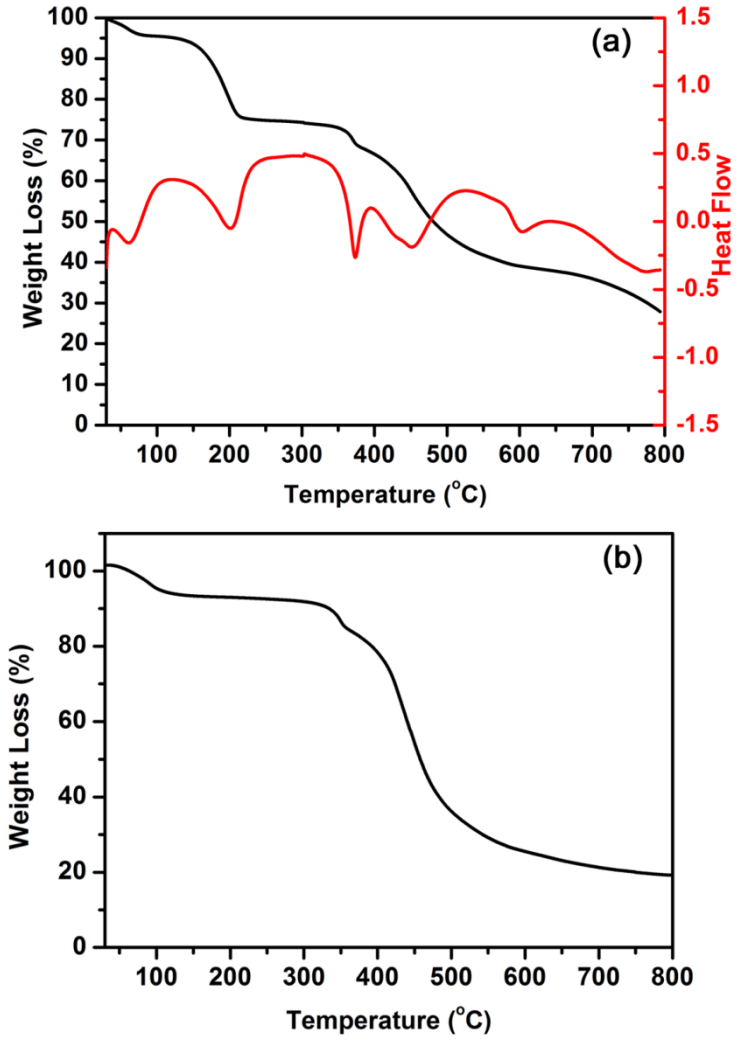

Figure S4. A view of (1, 1, -1) plane (blue) which go across the channel direction, the disappearance of this diffraction suggest the transformation of the open framework.